Centimeter-Wave Microstrip Phase Shifter on a Ferrite–Dielectric Substrate

SYLVAIN BOLIOLI, HAFED BENZINA, HENRI BAUDRAND, MEMBER, IEEE, AND B. CHAN

Abstract—**The propagation characteristics and fields of a microstrip transmission line on a composite ferrite–dielectric substrate are studied with a focus on its phase-shifting behavior. Two different methods are used for theoretical analysis, namely the least-squares boundary residual (LSBR), which offers high precision, and a variational method in the spectral domain, which requires a low computing time. Quasi-TEM propagation is assumed in both cases. The results obtained are compared with the experimental data, and good agreement is observed. Besides its easy design, this phase shifter presents the advantage of having a good peak power handling capacity as well as a low production cost because of the ease with which it can be integrated in planar systems.**

I. INTRODUCTION

THE DEVELOPMENT of phased-array antennas with two-plane electronic scanning in the centimeter-wave range depends largely on the miniaturization of the terminal phase shifters. In this paper, we propose the analysis of a composite microstrip dielectric–ferrite structure which fits well to such elements (Fig. 1). The dielectric layer reduces interaction between the electromagnetic wave and the ferrite beneath the microstrip conductor, the region where the magnetic field is the most important. It produces a better peak power handling capacity as well as a decrease in losses, but also entails a reduction of phase shifter efficiency.

The phase shifter will be described by its characteristic impedance and its maximum phase shift per unit length. The ferrite is magnetized longitudinally along the propagation axis O_z, thereby ensuring system reciprocity.

The quasi-TEM assumption, which we adopt here, implies small transverse dimensions in relation to the free-space wavelength; moreover, the propagating media are assumed to be lossless.

Consequently, and according to Green and Rado [1]–[4], the permeability tensor is of the form

$$\bar{\mu} = \mu_0 \cdot \begin{bmatrix} \mu & -jk & 0 \\ jk & \mu & 0 \\ 0 & 0 & \mu_z \end{bmatrix}$$

where μ, k, and μ_z are real quantities.

Manuscript received December 7, 1987; revised August 8, 1988

S. Bolioli and B. Chan are with O.N.E.R.A./C.E.R T./D.E.R.M.O., 2 avenue Edouard Belin, 31055 Toulouse Cedex, France.

H. Benzina and H. Baudrand are with E.N.S.E.E.I.H.T.-L.M.O., 2 rue Charles Camichel, 31071 Toulouse Cedex, France.

IEEE Log Number 8826052.

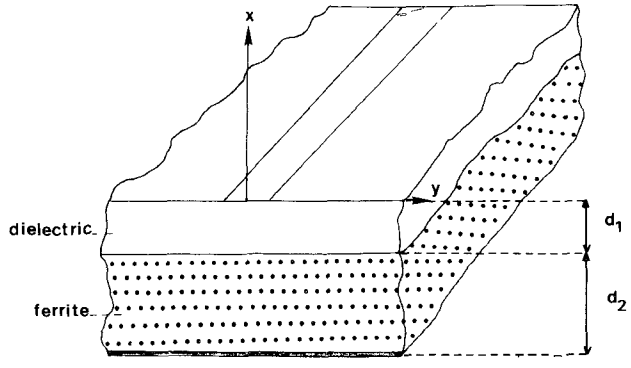

Fig. 1. Microstrip transmission line over a composite dielectric–ferrite substrate.

For the completely demagnetized state, μ_d, the expression of μ in this case is given by Schloemann's formula, calculated for a cylindrical sample:

$$\mu_d = \frac{1}{3}\left[1 + 2 \cdot \sqrt{1 - (\gamma 4\pi M_s / f)^2}\right]$$

where f = frequency, γ = gyromagnetic constant ($\gamma = 2.8$ MHz/Oe), and $4\pi M_s$ = saturation magnetization.

In the partially magnetized state, Green and Rado give experimental expressions for μ, k, and μ_z:

$$\mu = \mu_d + (1 - \mu_d)(4\pi M / 4\pi M_s)^{3/2}$$

$$k = \frac{\gamma 4\pi M_s}{f}$$

$$\mu_z = \mu_d \left[1 - (4\pi M / 4\pi M_s)\right]^{5/2}$$

where $4\pi M$ is the magnetization.

Based on these assumptions, two analysis methods are presented here, namely the variational approach in the spectral domain, developed by Yamashita [5] and Mittra [6], [7] for multilayer dielectric media, and the least-squares boundary residual (LSBR) method [8].

In the first, the characteristic impedance and the propagation constant are expressed in terms of the effective dielectric and magnetic constants. The ferrite is considered to be an isotropic medium with a scalar permeability μ_e derived from the tensor. The method consists in a variational calculation of line capacitance in the spectral domain. These approximations lead to a very short computa-

0018-9480/89/0400-0698$01.00 ©1989 IEEE

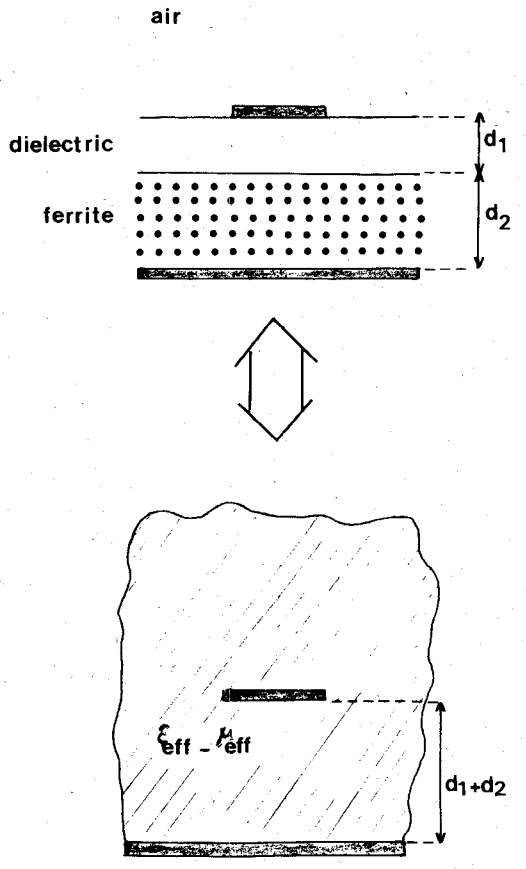

Fig. 2. Definition of effective electric and magnetic constants.

tion time (about 30 seconds on a personal computer) and fit well to a fast design of the device.

In the LSBR method, however, the ferrite anisotropy is conserved and the results are more accurate than those obtained by the variational one. Nevertheless, its numerical implementation is slightly more difficult and the computation is much longer. These two methods appear to be complementary.

II. Variational Method in the Spectral Domain

Let us consider the structure of Fig. 1, where the thickness of substrates and the strip width are small compared to the free-space wavelength; furthermore, the strip thickness is assumed to be zero. It is equivalent to a fictional transmission line containing a uniform medium of permeability μ_{eff} and permittivity ϵ_{eff} (Fig. 2). Therefore the propagation can be closely described by a plane wave in the TEM mode. Hence, we have transverse fields E and B, and the expression of the permeability tensor in the case of longitudinal magnetization leads to transverse H (this is not valid when the magnetization of the ferrite is perpendicular to the propagation axis).

According to these assumptions, the tensor can be reduced to the scalar transverse permeability:

$$\mu_e = \mu_T = \frac{\mu^2 - k^2}{\mu}.$$

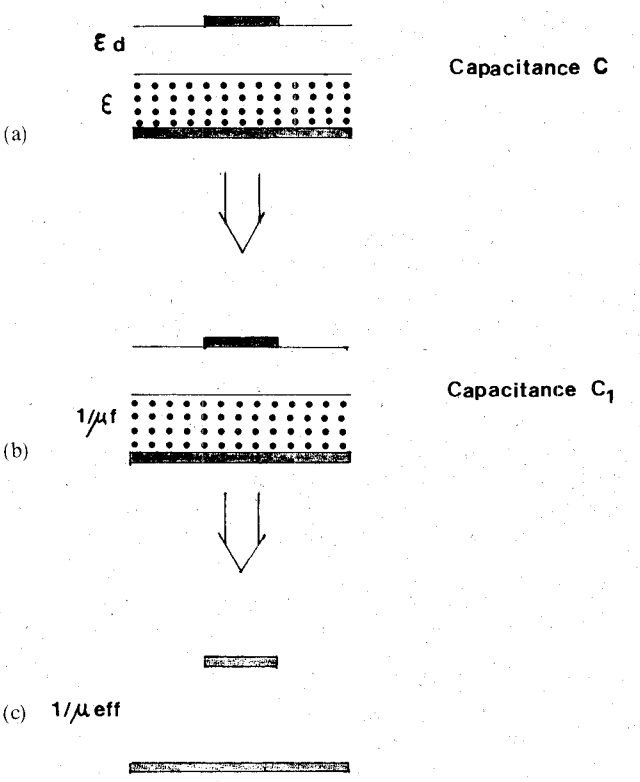

Fig. 3. Definition of effective permeability.

The characteristic impedance and the propagation constant can therefore be determined by means of the following formulas:

$$Z_c = \frac{\sqrt{\epsilon_{eff} \cdot \mu_{eff}}}{v \cdot C}$$

$$\beta = 2\pi f \cdot \frac{\sqrt{\epsilon_{eff} \cdot \mu_{eff}}}{v}$$

where C is the line capacitance per unit length, and v is the velocity of light. Thus, the transmission line is described by the capacitance C and by the effective permittivity ϵ_{eff} and permeability μ_{eff}.

If C_0 is the capacitance when the substrates are replaced by air, the effective dielectric constant is given by the ratio C/C_0. Similarly, the effective permeability can be obtained by considering the duality of ϵ and $1/\mu$ in Maxwell's equations as shown by Pucel and Masse [9]. First, the capacitance C_1 of a fictional transmission line is computed by replacing ϵ with $1/\mu_T$. The corresponding effective permeability is given by the ratio C_0/C_1 (Fig. 3). Thus the determination of Z_c and β is reduced to the computation of the different capacitances C_0, C, and C_1.

The variational expression of the line capacitance is given by [5], [10]

$$\frac{1}{C} = \frac{1}{Q^2} \int_{-\infty}^{+\infty} V(0, y) \cdot \rho(y) \cdot dy$$

where $\rho(y)$ is the surface charge density over the conductor, $V(x, y)$ is the transverse potential function, and Q is the total strip charge per unit length.

By using Parseval's formula, the above equation is transposed into the spectral domain:

$$\frac{1}{C} = \frac{1}{2\pi Q^2} \int_{-\infty}^{+\infty} \tilde{V}(0, p) \cdot \tilde{\rho}(p)\, dp$$

where $\tilde{V}(0, p)$ and $\tilde{\rho}(p)$ are the Fourier transforms of $V(0, y)$ and $\rho(y)$, respectively. $\tilde{V}(0, p)$ can be expanded by using the Fourier transform of the Green's function over the conductor, which gives

$$\frac{1}{C} = \frac{1}{2\pi Q^2} \int_{-\infty}^{+\infty} \tilde{G}(0, p) \tilde{\rho}^2(p)\, dp.$$

$\tilde{G}$ is obtained by solving Poisson's equation under the quasi-TEM assumption, transposed into the spectral domain, and by solving the electric field continuity conditions at the different interfaces. Its expression over the strip is given in the Appendix.

On the other hand, in order to calculate the charge density, ρ, we can assume that the conductor potential is constant and equal to V_0. This leads to the following relationship:

$$V_0 = V(0, y) = \int_{\text{conductor}} G(y, y') \rho(y')\, dy'$$

$$\text{for } |y| < W/2.$$

This is a Fredholm equation of the first kind where $\rho(y')$ is the unknown, and the point-matching technique is applied for its resolution. The charge density ρ is decomposed into $2N$ rectangular basis functions (see Fig. 4):

$$\rho(y) = \begin{cases} R_i & \text{for } y_{i-1} < |y| < y_i \\ 0 & \text{for } |y| > w/2. \end{cases}$$

The convolution by the Green's function being a linear operator, the expression of the potential function on the strip conductor in the spectral domain becomes

$$V_0 = \int_{-\infty}^{+\infty} \tilde{G}(0, p) \cdot e^{jpy_i} \tilde{\rho}(p)\, dp \qquad \text{for } i = 1, 2, \cdots, N.$$

In this way, a linear system is obtained where the R_i's can be deduced from the V_0. It suffices then to substitute them into the capacitance expression.

III. Least-Squares Boundary Residual Method

The LSBR method has been successfully applied to certain electromagnetic problems, in particular those which involve the wave propagation and radiation in planar structures [11], [12]. The main difficulty is choosing a numerical technique that will allow the optimization of factors such as the computation time and memory storage.

Usually, according to the different variants of this method, a reduced computer memory storage leads to a longer computation time and vice versa. In spite of its tedious numerical implementation, the LSBR method seems to be quite satisfying as far as accuracy is concerned.

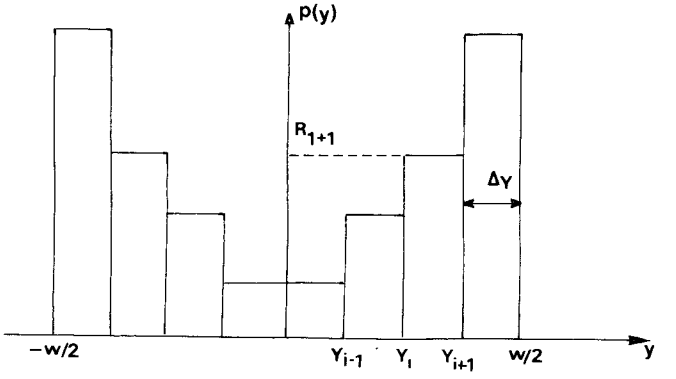

Fig. 4. Rectangular basis function of ρ.

Here, we have applied this method to analyze a structure through the use of one of its variants, which consists in changing the basic functions [8].

The quasi-TEM assumption allows the propagation characterization by calculating only the capacitance and the inductance of the structure's cross section. The main idea consists in expanding the electrostatic and magnetostatic potentials V and U into harmonics; then the electric and magnetic fields E and H are respectively derived from them.

Once the field expressions are obtained, the boundary conditions at the interfaces are applied, and on the conductor interface we can obtain the following expressions. For the electrostatic case,

$$\mathcal{N}_i\big(n \cdot [D_2(0, y) - D_1(0, y)]\big) + \mathcal{N}_m\big(n \cdot E(0, y)\big) = 0.$$

For the magnetostatic case,

$$\mathcal{N}_i\big(n \cdot [H_2(0, y) - H_1(0, y)]\big) + \mathcal{N}_m\big(n \cdot B(0, y)\big) = 0.$$

Here

$$\mathcal{N}_m = \begin{cases} 1 & \text{along the conductor width} \\ 0 & \text{elsewhere} \end{cases}$$

$$\mathcal{N}_i = 1 - \mathcal{N}_m$$

and

$$D_e = \epsilon_e E_e \qquad B_e = \bar{\bar{\mu}}_e H_e, \qquad e = 1, 2, 3.$$

These equations can be rewritten in the following forms:

$$\mathcal{N}_i \rho(y) + \mathcal{N}_m \cdot E_y(y) = 0 \qquad \text{electrostatic case}$$

$$\mathcal{N}_i j(y) + \mathcal{N}_m \cdot B_x(y) = 0 \qquad \text{magnetostatic case}$$

where $j(y)$ is the surface current density.

We now put them in the general form

$$\mathcal{N}_i f(y) + \mathcal{N}_m A(y) = 0.$$

The truncation of the two series functions $f(y)$ and $A(y)$ leads to a functional $\phi(y)$, written as

$$\phi(y) = \mathcal{N}_i f(y) + \mathcal{N}_m A(y).$$

The LSBR method consists then in minimizing the following expression:

$$\langle \phi(y) | \phi(y) \rangle = \int_{-b/2}^{+b/2} \phi^t(y) \cdot \phi(y)\, dy$$

where b is the distance between the two lateral electric walls. It can be shown that $f(y)$ and $A(y)$ can be expressed as

$$f(y) = \sum_{n=-\infty}^{+\infty} G_n(y) \cdot Y_n$$

$$A(y) = \sum_{n=-\infty}^{+\infty} G_n(y) \cdot K_n \cdot Y_n$$

with

$$G_n(y) = 1/\sqrt{b}\, e^{jn\beta y} \quad \text{and} \quad \beta = 2\pi/b.$$

Before proceeding to the basis function change, it is interesting to note that the combination of the two previous equations (electrostatic and magnetostatic cases) yields

$$\mathcal{N}_i f(y) + \mathcal{N}_m \sum_{n=-\infty}^{+\infty} |G_n(y)\rangle K_n \langle G_n(y)|f(y)\rangle = 0.$$

Moreover

$$\hat{L} f(y) = 0$$

where $\hat{L}$ is a linear operator and

$$\hat{L} = \mathcal{N}_i \cdot \hat{I} + \mathcal{N}_m \sum_{n=-\infty}^{+\infty} |G_n(y)\rangle K_n \langle G_n(y)|$$

$\hat{I}$ being the identity operator.

If L_N denotes the truncated operator up to a finite number N, the problem will consist in minimizing the following form:

$$\langle f(y)|\hat{L}_N^t \hat{L}_N|f(y)\rangle$$

where the superscript t denotes the adjoint operator.

We have chosen rectangular pulses as the new basis functions T_p defined only over the conductor, such that

$$T_p = \begin{cases} 1/\sqrt{p} & \text{for } y_p - \delta/2 \leqslant y \leqslant y_p + \delta/2 \\ 0 & \text{elsewhere.} \end{cases}$$

Here $y_p = p \cdot \delta$, and $\delta = W/\text{number of basis functions}$. Then $f(y)$ is rewritten as

$$f(y) = T_p(y) \cdot Y_p.$$

The expression to be minimized becomes

$$\langle Y|A|Y\rangle = \sum_q \sum_m \sum_n \sum_p Y_q^t S_{m,q}^t K_m^t \cdot \langle G_m(y)|\mathcal{N}_m|G_n(y)\rangle K_n S_{n,p} Y_p$$

where $S_{i,j} = \langle G_i(y)|T_j(y)\rangle$, and A is a definite positive matrix.

In order to avoid the trivial solution $Y = 0$, we impose the condition

$$\langle Y|Y\rangle = 1.$$

The solution is the eigenvector Y corresponding to the smallest eigenvalue of A.

Now, we present the different steps in the solution of our problem concerning the structure of Fig. 5.

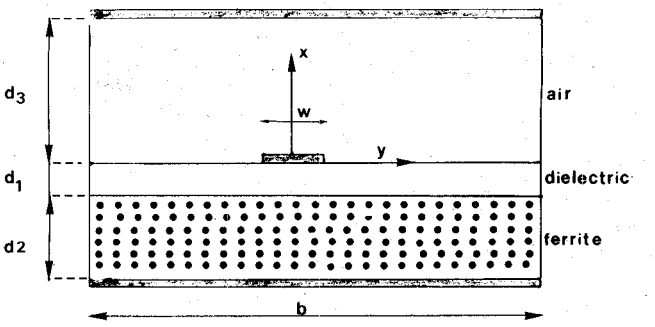

Fig. 5. Shielded structure for the study with the LSBR method.

A. Electrostatic Analysis

The electrostatic potential V is the solution of Laplace's equation:

$$\left[\frac{\partial^2}{\partial x^2} + \frac{\partial^2}{\partial y^2}\right] V = 0.$$

The solution is found to be

$$V^i(x, y) = \sum_{n=-\infty}^{+\infty} \left[A_n^i e^{|n\beta|x} + B_n^i e^{-|n\beta|x}\right] e^{jn\beta y}$$

where $i = 1, 2, 3$ denotes the different media.

The previous general equation can be written as

$$\sum_{n=-\infty}^{+\infty} \left[\mathcal{N}_m K_n^e + \mathcal{N}_i\right] \cdot Y_n^e G_n(y) = 0$$

with superscript e indicating the electrostatic case. The full expression of K_n^e is given in the Appendix.

The total charge Q is obtained by integrating the surface charge density $\rho(y)$ over the conductor width:

$$Q = \int_{\text{strip}} \rho(y)\, dy = \int_{\text{strip}} \sum_p Y_p^e T_p(y)\, dy = \sqrt{\delta} \sum_p Y_p^e.$$

The potential V can be expressed in terms of the eigenvector components as

$$V = \frac{2}{b\sqrt{\delta}} \sum_n \sum_p \frac{K_n \cdot Y_n^e \cdot S_{n,p}}{n\beta}.$$

By having the charge and potential values, the capacitance is deduced immediately:

$$C = Q/V.$$

B. Magnetostatic Analysis

The magnetostatic potential U is the solution of Laplace's equation:

$$\left[\frac{\partial^2}{\partial x^2} + \frac{\partial^2}{\partial y^2}\right] U = 0.$$

The solution is found to be

$$U^i(x, y) = \sum_{n=-\infty}^{+\infty} \left[C_n^i e^{|n\beta|x} + D_n^i e^{-|n|x}\right] e^{jn\beta y}.$$

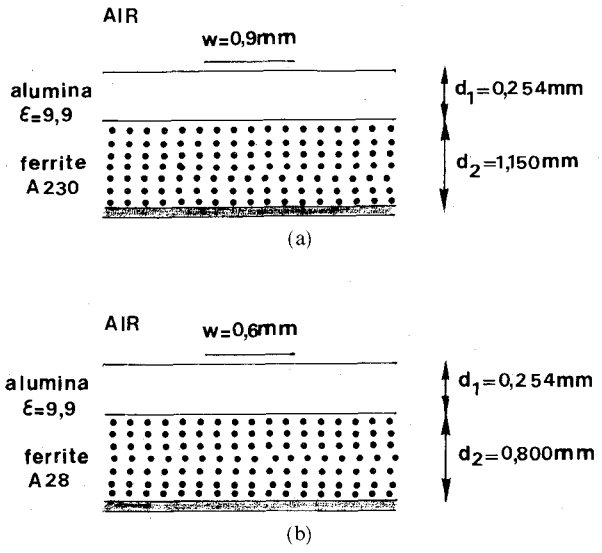

Fig. 6. Cross sections of experimental phase shifters.

The general equation can be written as

$$\sum_{n=-\infty}^{+\infty} \left[\mathcal{N}_m K_n^h + \mathcal{N}_i\right] Y_n^h G_n(y) = 0$$

where the superscript h indicates the magnetostatic case. The full expression of K_n^h is given in the Appendix.

Similarly the current I is obtained by integrating the surface charge density $j(y)$ over the conductor width:

$$I = \int_{\text{strip}} j(y)\, dy = \int_{\text{strip}} \sum_p Y_p^h T_p(y)\, dy = \sqrt{\delta} \sum_p Y_p^h.$$

The magnetic induction flux φ through the (y, z) plane between the conductor edge and the lateral wall can be calculated as

$$\varphi = \int_{w/2}^{b/2} \mu_0 H_x(0, y)\, dy$$

and the inductance L is determined as

$$L = \varphi / I.$$

In this way, the propagation constant and the characteristic impedance are determined by the classical transmission line equations.

The fields can be calculated at the dielectric–ferrite interface using the eigenvector components in the new basis.

IV. Application to Phase Shifters

We present here the experimental results concerning two phase shifter prototypes, realized by using the following Thomson/CSF ferrites (Fig. 6(a) and (b)):

FERRITE	A230	A28
ϵ' ($\epsilon = \epsilon' + j\epsilon''$)	16,6	16,6
$4\pi M_s$ (gauss)	2300	2800
$4\pi M_{\max}$ (gauss)	1740	2240

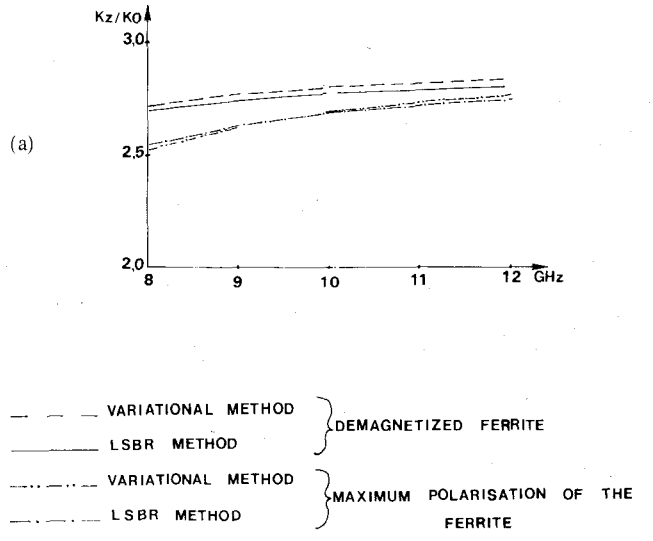

Fig. 7. (a) Normalized propagation constant versus frequency (A230). (b) Characteristic impedance versus frequency (A230).

A. Propagation Constant and Characteristic Impedance

The two methods have been applied for the design of the phase shifters, and Figs. 7 and 8 show the excellent agreement between the theoretical results. The maximum difference between the obtained values is 2 percent for the characteristic impedance in the case of maximum polarization, less than 1 percent for that of the demagnetized structure, and 1 percent for the propagation constant.

The calculation of the microstrip width W corresponding to a characteristic impedance of 50 Ω gives 0.9 mm for the A230 structure and 0.67 mm for the other one, where the operating frequency is 10 GHz. Figs. 9(a) and 10(a) illustrate the measured SWR in the 8–12 GHz band, where it is less than 1.2 everywhere (under −20 dB), except below 9 GHz for the A28 phase shifter, where losses appear in the low magnetic field zone. The polarization induction is created by a 2000-turn solenoid around the phase shifter.

B. Phase Shift

The diagrams of Figs. 9(b) and 10(b) show the experimental differential phase shift between the polarized and demagnetized states as a function of the magnetization (i.e., the current in the solenoid).

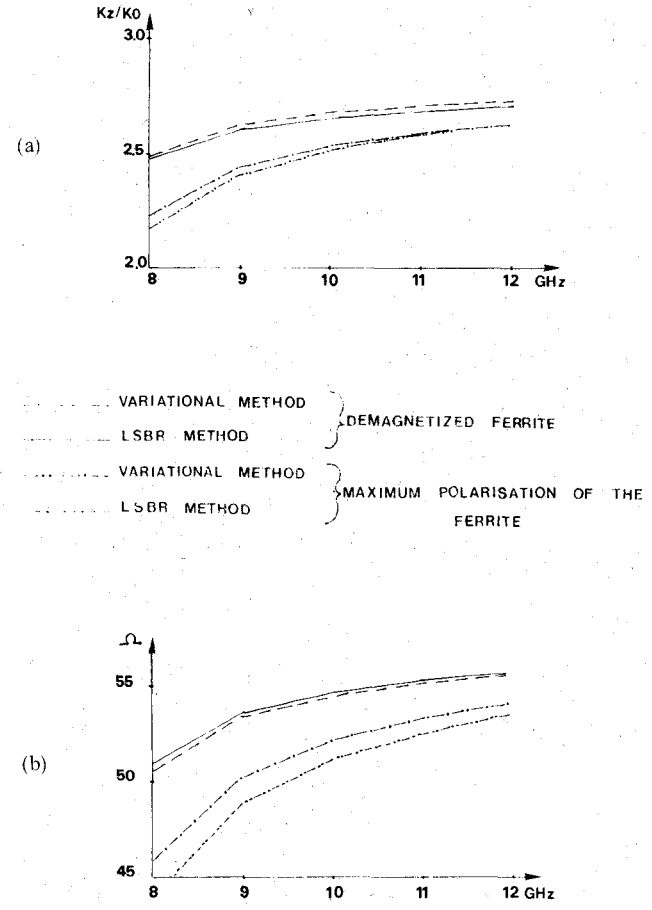

Fig. 8. (a) Normalized propagation constant versus frequency (A28). (b) Characteristic impedance versus frequency (A28).

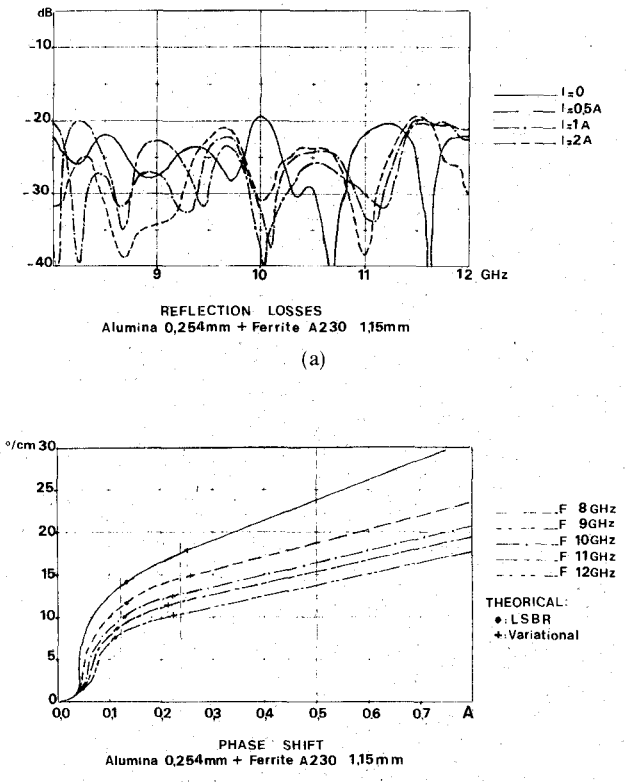

Fig. 9. Composite line: experimental results (A230).

The predicted phase shift is calculated for a saturated ferrite, below the limit where nonlinear phenomena appear. This state is characterized by the end of the saturation bend yielding a nearly linear curve, and corresponds, respectively, to 100 mA and 500 mA through the solenoid in the A230 and A28 cases. The LSBR method gives results which are nearer to this definition. However, it is interesting to note that, in both cases, the theoretical values are in good agreement with the experimental ones, around well-defined polarization levels (120 mA and 500 mA for the LSBR method, 230 mA and 800 mA for the variational one).

C. Magnetic Field Distribution

In order to complete the structure characterization, the magnetic field distribution has been determined by both methods for the A230 phase shifter. The variations of the tangential and normal components of H in the dielectric and at the ferrite–dielectric interface are presented in Fig. 11(a) and (b). We note that LSBR method gives higher values of H than the variational one.

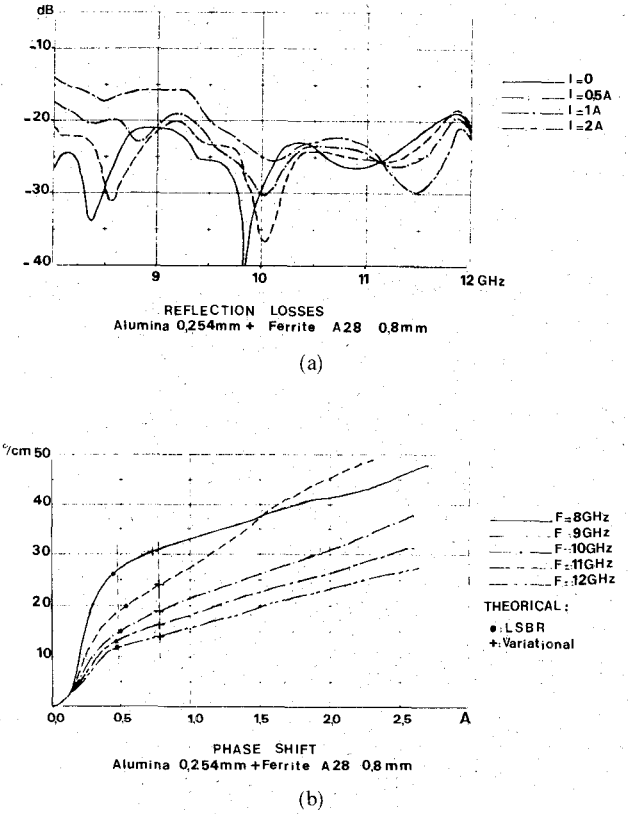

Fig. 10. Composite line: experimental results (A28).

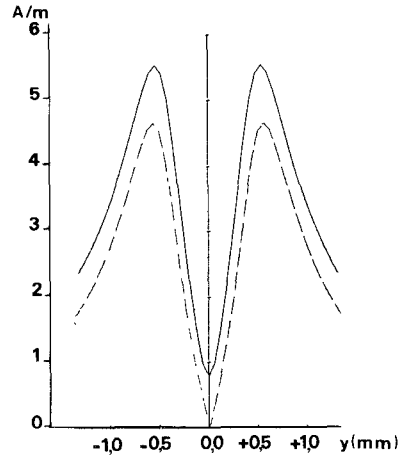

(a)

LSBR method···Tensorial magnetic permeability
—.—.—.—Variational method···Effective magnetic permeability

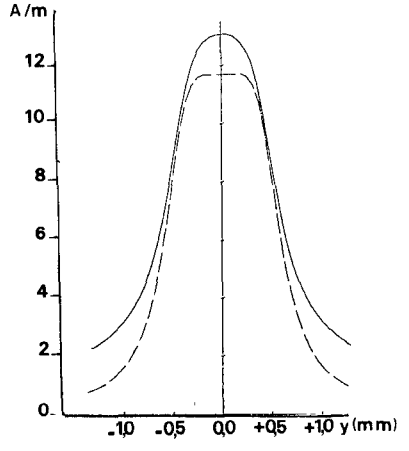

(b)

Fig. 11. (a) Normal component of H. (b) Tangential component of H.

V. Conclusion

A variational method in the spectral domain and the LSBR method have been applied successfully to the analysis of composite ferrite–dielectric microstrip phase shifters. In each case, the elaborated computer program has undergone several validation tests, and very good agreement has been observed between theoretical and experimental results. Moreover, the design of such phase shifters is very easy, and optimizations can be considered, leading to their use in two-plane electronically scanned antennas.

Appendix

1) Expression of the Fourier Transform of the Green's Function over the Strip for the Variational Method:

$$G(0,p)=\frac{1}{p\epsilon_0}\cdot\frac{\epsilon_1 th(pd_2)+\epsilon_2 th(pd_1)}{\epsilon_2[\epsilon_1+\epsilon_2 th(pd_1)th(pd_2)]+[\epsilon_1 th(pd_2)+\epsilon_2 th(pd_1)]}.$$

2) Expression of K_n^e in Electrostatic Case for LSBR:

$$K_n^e=\frac{1}{\epsilon_0}\cdot\frac{S_n N th(|\beta n|d_3)}{N+\epsilon_1 th(|\beta n|d_3)[\epsilon_2+\epsilon_1 th(|\beta n|d_1)th(|\beta n|d_2)]}$$

with

$$N=\epsilon_2 th(|\beta n|d_1)+\epsilon_1 th(|\beta n|d_2)$$

and

$$S_n=|n|/n.$$

3) Expression of K_n^h in Magnetostatic Case for LSBR:

$$K_h^h=\frac{S_n N th(|\beta n|d_3)}{th(|\beta n|d_1)+th(|\beta n|d_3)}\cdot\frac{N_1+N_2 th(|\beta n|d_2)}{D_1+D_2 th(|\beta n|d_3)}.$$

N and S_n are the same as above. In addition,

$$D_1=\mu_0\mu|\beta n|^2$$

$$N_1=D_1\cdot th(|\beta n|d_1)$$

$$D_2=\frac{(\mu^2-k^2)(\beta n)^2}{th[|\beta n|(d_1+d_3)]}-\mu_0 k\beta n|\beta n|$$

$$N_2=(\mu^2-k^2)(\beta n)^2-\mu_0 k\beta n|\beta n| th(|\beta n|d_1).$$

References

[1] J. J Green, "Microwave properties of partially magnetized ferrites," R.A.D.C. TR 68 312, Final Report, Aug. 1968, Rome Air Development Center, A.F.S.V.-G.A.F.B., NY.

[2] J. J. Green, E. Schlomann, F. Sandy, and J. Saunders, "Characterization of the microwave tensor permeability of partially magnetized materials," R.A.D.C TR 6963, Feb. 1969, Rome Air Development Center, A.F.S.V.-G.A.F.B., NY.

[3] F. J. Rosenbaum, "Integrated ferrimagnetic devices," in *Advances in Microwaves*, vol. 8 New York: Academic Press, 1974.

[4] S. Bolioli, "Déphaseur à structure composite ferrite diélectrique en ondes centimétriques," Thése Docteur Ingénieur E.N.S.A.E., Toulouse, France, 1984.

[5] E. Yamashita, "Variational method for the analysis of microstrip-like transmission lines," *IEEE Trans. Microwave Theory Tech.*, vol. MTT-16, Aug. 1968.

[6] R. Mittra and T. Itoh, "Analysis of microstrip transmission lines," in *Advances in Microwaves,* vol 8. New York: Academic Press, 1974.

[7] R. Mittra, *Computer Techniques for Electromagnetic.* Elmsford, NY: Pergamon Press.

[8] H. Baudrand, M. Boussouis, J. L. Amalric, "Analysis of some planar structures by the least-squares boundary residual method," *IEEE Trans. Microwave Theory Tech.*, vol. MTT-34, Feb. 1986.

[9] R. A. Pucel and D. J. Masse, "Microstrip propagation on magnetic substrates—Part I: Design theory," *Microwave Integrated Circuits.* Norwood, MA: Artech House, 1975.

[10] E. Yamashita and K. Atsuki, "Stripline with rectangular outer conductor and three dielectric layers," *IEEE Trans. Microwave Theory Tech.*, vol. MTT-18, May 1970.

[11] J. B. Davies, "A least-square boundary residual method for numerical solution for scattering problems," *IEEE Trans. Microwave Theory Tech.*, vol. MTT-21, Feb. 1973.

[12] R. Jansen, "A modified least-squares boundary residual (L.S.B.R) method and its application to the problem of shielded microstrip dispersion," *Arch. Elek. Übertragung.*, Band 28, Heft 6, 1974.

[13] T. G. Bryant and J. A. Weiss, "Parameters of microstrip transmission lines and of coupled pairs of microstrip lines," *IEEE Trans. Microwave Theory Tech.*, vol. MTT-16, Dec. 1968.

[14] E. R. B. Hansson, S. Aditya, and M. Larsson, "Planar meander ferrite-dielectric phase-shifters," TR 8004, Chalmers University of Technology, Gothenburg, Sweden, May 1980

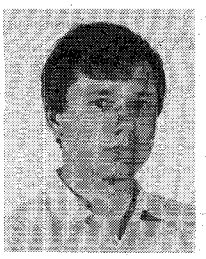

Sylvain Bolioli was born in Italy in 1959. He received the Diplôme d'Ingénieur in electronics from E.N.S.E.E.I.H.T. in 1982 and the Docteur-Ingénieur degree from the Ecole Nationale Supérieure de L'Aéronautique et de l'Espace, Toulouse, France, in 1984.

Since 1985, he has been engaged in research on microwave and millimeter-wave phase shifters with the Centre d'Etudes et de Recherches de Toulouse.

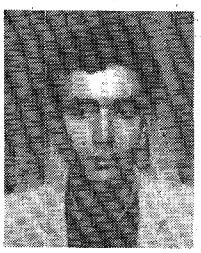

Hafed Benzina was born in Gabes, Tunisia, in 1961. He obtained the Maitrise es Sciences Physiques degree from the Faculté des Sciences, Tunis University, Tunisia. He is currently working toward the Ph.D. degree at the Institut National Polytechnique, Toulouse, France, at the Laboratoire de Micro-Ondes of E.N.S.E.E.I.H.T. His research interests include analytical and numerical methods for solving electromagnetic problems.

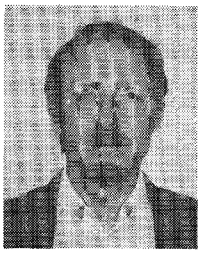

Henri Baudrand (M'86) was born in 1939. He obtained the Diplôme d'Ingénieur in electronics and the Docteur-es-Sciences degree in microwaves, both from E.N.S.E.E.I.H.T., in Toulouse, France, in 1962 and 1966, respectively.

He is a Professor at the Institut National Polytechnique, Toulouse, France, in microwaves, electromagnetism, and semiconductor physics. His field of research is the modeling of active and passive microwave components. He has more than 100 publications and presentations at conferences.

B. Chan, photograph and biography not available at the time of publication.